Hydrologic Performance of Permeable Pavement as an Adaptive Measure in Urban Areas: Case Studies near Montreal, Canada

Catherine Vaillancourt[1]; Sophie Duchesne, Ph.D.[2]; and Geneviève Pelletier, Ph.D.[3]

Abstract: The infiltration capacity of permeable interlocking concrete pavement (PICP) was characterized on five sites located in the greater Montreal area (Canada). Surface infiltration rates up to more than 20,000 mm/h were observed, even in winter at subzero temperatures (°C). At one of the five monitored sites, rainfall and flow at the outlet were monitored for 12 months. This monitoring revealed peak flow delays ranging from 4 min to 4 h 42 min and runoff reductions ranging from 26% to 98%, depending on the rainfall event. These rainfall and flow data were used to calibrate a PICP hydrologic model that was then used to quantify the impact of implementing PICP in four real urban watersheds. For an eight-year rainfall series, simulations showed a reduction in volume (65%) and duration (21%–48%) of overflows in the two combined sewer systems, a reduction in peak flow (6%–45%) and volume (mean 30%) at the outfall of the two separate systems, and a reduction in surface flooding duration (24%–81%) for the four sewer systems. **DOI: 10.1061/(ASCE)HE.1943-5584.0001812.**

Introduction

The increase in impervious surfaces due to urbanization causes significant changes to the hydrologic cycle in urban areas. These changes include not only increased peak flows and runoff, but also reduced groundwater recharge (Aryal et al. 2016). These impacts can have consequences on drainage system performance, such as more frequent and greater storm sewer backups (Huong and Pathirana 2013), and on the water quality of streams (Hatt et al. 2004), consequences that are exacerbated by changes in precipitation patterns associated with climate change (Neumann et al. 2015). There are various solutions for mitigating the negative impact of urbanization on infrastructure and watercourses, including source control solutions, which contribute to the retention, infiltration, and/or evaporation of runoff before it enters the storm sewer system. Among the most common source control systems are rain gardens or bioretention systems, vegetative swales, filter strips, vegetated roofs, disconnected roof downspouts, rain barrels, separators (hydrodynamic or other), and permeable pavement and other types of pervious surfaces. These systems are designed to help runoff infiltrate the soil and, in some cases, to temporarily retain runoff. Permeable pavement can be continuous (pervious concrete, porous asphalt, and recycled material surfaces), discontinuous (porous pavers and permeable interlocking concrete pavement), open (flagstones and geogrids) or loose (porous gravel and porous turf). All types of permeable pavements can replace impervious surfaces without sacrificing land use (Drake et al. 2013). They are suitable for public parking lots and residential driveways and also for low traffic volume roads.

Permeable interlocking concrete pavement (PICP) is a particular type of discontinuous permeable pavement consisting of impervious concrete pavers that are designed to interlock. They are separated by joint filling materials that have a sufficiently high porosity to allow water to quickly infiltrate the surface (ICPI 2007). The water then goes into a reservoir layer with a large void volume for collecting and retaining the water. If the soil is too impervious to allow all the water to infiltrate, a perforated underdrain is added to the reservoir layer to help evacuate excess water toward the storm sewer system (Eisenberg et al. 2015). Keeping the joints filled with granular material, avoiding the input of sediments from adjacent surfaces, and cleaning the surfaces regularly can help maintain a high infiltration rate into the PICP reservoir layer. Brushes or street sweepers can be used to restore the infiltration capacity of joints when they are clogged with fine sediment. For more severe clogging, usually due to poor maintenance, interjoint material can be removed by vacuum sweepers and replaced with clean material.

Drake et al. (2013) conducted an exhaustive scientific literature review of the environmental performance of permeable pavements. The review included a summary of conclusions on hydrologic performance, on impacts on water quality, and on the longevity, functionality, and maintenance needs of permeable pavement systems. With regard to impacts on water quality, the removal rate of suspended solids (SS) and metals through this type of system was studied by Fassman and Blackbourne (2007, 2011), Pratt et al. (1989, 1995), Beecham et al. (2012), Drake et al. (2014b), and Huang et al. (2012). These studies concluded that water quality improved, because the permeable pavements captured pollutants. These authors found that the concentration of suspended solids and heavy metals was reduced by at least 50% when stormwater filtered through permeable pavements. With regard to hydraulic performance, Abbott and Comino-Mateos (2003), Collins et al. (2008), Fassman and Blackbourn (2010), Pratt et al. (1989, 1995), TRCA (2008), Huang et al. (2012), Drake et al. (2012, 2014a), and Kim et al. (2015) all showed, for various individual cases, that

[1]Engineer, Eau Terre Environnement Research Centre, Institut National de la recherche scientifique, 490 Couronne St., QC, Canada G1K 9A9; presently, Quebec Ministry of Environment and Fight Against Climate Change, 100 Industriel Blvd., Repentigny, QC, Canada J6A 4X6.

[2]Professor, Eau Terre Environnement Research Centre, Institut National de la recherche scientifique, 490 Couronne St., QC, Canada G1K 9A9 (corresponding author). Email: sophie.duchesne@ete.inrs.ca

[3]Professor, Dept. of Civil and Water Engineering, Laval Univ., QC, Canada G1V 0A6.

Note. This manuscript was submitted on November 8, 2018; approved on March 12, 2019; published online on June 8, 2019. Discussion period open until November 8, 2019; separate discussions must be submitted for individual papers. This paper is part of the ***Journal of Hydrologic Engineering***, © ASCE, ISSN 1084-0699.

permeable pavements help reduce peak flow rate and runoff volume in storm sewer systems during rainfall events. Among these authors, only Drake et al. (2012, 2014a), Huang et al. (2012), and TRCA (2008) demonstrated these effects in a harsh winter climate, with winter thaws, such as those occurring in the southern parts of Canada. Other permeable pavement benefits mentioned in the literature include reducing the effects of heat islands (Eisenberg et al. 2015) and lowering the temperature of the runoff released into the natural environment (Wardynski et al. 2013).

More specifically, with regard to PICP, the fact that only the joints and not the pavers are permeable increases PICP's resistance to cold (Thelen and Howe 1978). Furthermore, the highly porous subbase limits frost heave, increasing the pavers' durability. PICP also allows surfaces to continue being used even during intense rainfall events, because water quickly seeps through the pavement and does not form puddles. For the same reason, PICP helps prevent surface ice from forming in the winter, which means that abrasives and deicing salt do not need to be applied. Several recent studies evaluated the reduction in surface runoff volume (Wardynski et al. 2013; Huang et al. 2016; Winston et al. 2018; Braswell et al. 2018; Hu et al. 2018) and peak flow rates (Huang et al. 2016; Hu et al. 2018) when using PICP. In addition to these studies, many more have aimed at assessing the impact of PICP on water quality. In particular, research conducted by Winston et al. (2016), Brown and Borst (2015), and Drake et al. (2014b) involved PICP sites in cold climates. These studies found significant improvements in water quality by capturing SS and reducing nutrients. All of these studies, except that of Hu et al. (2018), were conducted at a site scale. The performances observed suggest that implementing PICP on a larger scale in urban areas would help improve the hydrologic behavior of systems and reduce the impact of urbanization on the receiving environment. To our knowledge, only Hu et al. (2018) has evaluated the impact of PICP at an urban subwatershed scale; however, the study was limited, because the model was not calibrated and a single event was used as input to the model.

In this context, the main objective of this study was to assess the performance of permeable pavements at an urban watershed scale with regard to (1) protecting receiving bodies of water (peak flow rates and velocities, released volumes) and (2) reducing hydraulic dysfunctions (surface flooding due to surcharges) in storm sewer systems. These assessments were conducted in real urban sectors based on a hydrologic/hydraulic model integrating a calibrated permeable pavement module using rainfall and flow rate observations from a real PICP site.

Methodology

To reach the aforementioned main objective, a five-step method was applied: (1) characterization of the infiltration capacity of PICP; (2) field observations and water balance at an instrumented PICP site; (3) hydrologic modeling of the instrumented site's operation; (4) design improvement; and (5) modeling of real urban areas and impact assessment. In all cases, the permeable pavement used was the Inflo technology from Techo-Bloc (Chambly, Canada), which consists of a PICP layer over a subbase storage layer composed of gravel, as shown in Fig. 1(a). The cost involved for the construction of this kind of infrastructure varies from site to site, but is on the order of 200 $\mathrm{CAD/m^2}$ (materials and labor), including the pavers, bedding layer, foundation, subfoundation, borders, and geotextile. The design of such PICP sites is usually performed in two steps, the hydrologic design and the structural design. The final dimensions are selected to meet the requirements of both designs. For the structural design, engineers can refer to the manual recently published by ASCE (2018).

Characterization of the Infiltration Capacity of PICP

Infiltration capacity was measured at five sites in the greater Montreal area (Quebec, Canada) where the Inflo technology was installed. Site characteristics are briefly described in Table 1. These sites, built between 2011 and 2014, support varying levels of traffic, ranging from light to heavy truck traffic (at the TB site). Infiltration capacity was measured in three different locations at each site, from two to five times between August 2015 and June 2016. The temperature during the tests ranged from −14°C to 32°C. The infiltration capacity was assessed according to ASTM C1781/C1781M-14a (ASTM 2015)—an infiltration ring was sealed to the surface of the pavement to determine the in situ surface infiltration capacity of the permeable pavement with joints.

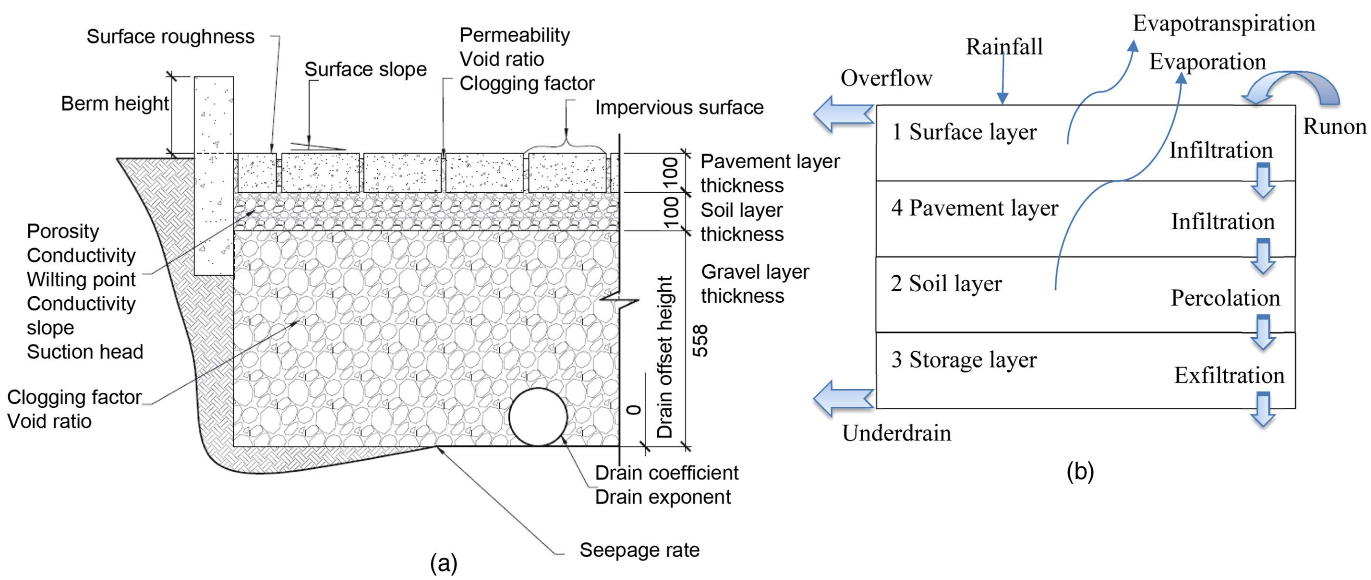

Fig. 1. (a) PICP design and modeling parameters; and (b) representation in the LID module in SWMM (adapted from Rossman and Huber 2016).

J. Hydrol. Eng., 2019, 24(8): 05019020

Table 1. Site characteristics and infiltration capacity (mm/h)

Site	Construction	Land use	Surface area (m^2)	Sample	August 2015	October 2015	November 2015	February 2016	May–June 2016
TB	2011	Industrial: road access for trucks and storage	28,160	TB 1	121	698	1,056	2,101	1,027
				TB 2	2,176	2,104	1,385	1,335	1,490
				TB 3	1,654	2,739	1,338	3,775	—
PP	2012	Parking	≈2,000	PP 1	5,098	3,746	5,166	—	1,648
				PP 2	5,460	5,808	3,460	—	5,645
				PP 3	4,907	7,939	4,695	—	7,974
SM	2013	Emergency road: infrequent use; snow removed in winter	≈800	SM 1	2,369	7,383	1,382 (snow)	—	—
				SM 2	1,258	770	697 (snow)	—	—
				SM 3	3,485	1,532	Too cold to seal ring	—	—
RV	2014	Parking	≈400	RV 1	5,586	6,052	3,308 (snow)	—	2,327
				RV 2	1,454	2,324	1,591 (snow)	—	2,950
				RV 3	7,603	9,471	Too cold to seal ring	—	9,043
UD	2013	Access road to school parking	≈150	UD 1	—	—	—	—	2,014
				UD 2	—	—	—	—	2,184
				UD 3	23,121	18,065	Too cold to seal ring	—	1,687

Note: TB = Techo-Bloc; PP = Patriots Park; SM = Saint-Martin; RV = Residences Vimont; and UD = Ulric-Debien.

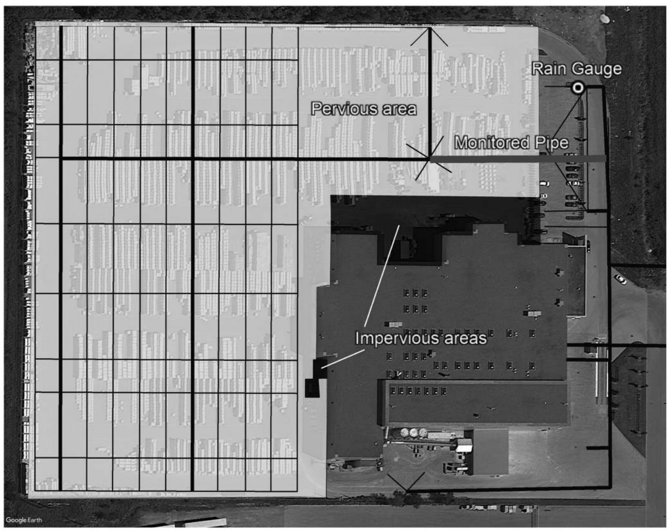

Fig. 2. TB site layout—pervious (light gray) and impervious (dark gray) areas. (Image © Google.)

Field Observations and Water Balance at an Instrumented PICP Site

The TB site (Fig. 2) was instrumented for three seasons (September 2015–January 2016; June–December, 2016; April–September, 2017). The rear storage yard of this site consists of an area of 28,160 m^2, of which 1,585 m^2 are impervious and 26,575 m^2 are permeable (PICP). In Fig. 2, the area close to the building (dark shading) is impervious (the pavement joints were sealed to protect the building against water infiltration), whereas the joints are permeable elsewhere (light shading). The pavers forming the surface are made of impervious concrete; they are rectangular (200×300 mm), 100 mm thick, and separated by 13-mm joints filled with 2.5–10 mm diameter fine aggregate (in the permeable part). Under the layer of pavers is a base consisting of 100 mm of gravel (5–14 mm in diameter) with a subbase of 508 mm of gravel (25–75 mm in diameter). A filtering geotextile separates the subbase from the existing soil subgrade. The gravel base is drained by a dense system of 150-mm diameter perforated high-density polyethylene (HDPE) pipes surrounded by porous geotextile and installed directly on the subbase.

A tipping bucket rain gauge (the RG3-M model from Onset with a 0.2-mm resolution, Bourne, Massachusetts) was installed at the front of the site (see Fig. 2). The rain gauge recorded the time and date of each bucket tip. These recordings were converted into rainfall depth at 1-min intervals with the filter tool of the HOBOware software version 3.7.10 supplied with the rain gauge. A MantaRay flowmeter from Greyline (Long Sault, Ontario) was installed in the outlet (monitored pipe) shown in Fig. 2. The flowmeter continuously measured water velocity and depth using the Doppler principle in order to estimate flow, either in open channel or surcharge conditions. According to the manufacturer, the device has an accuracy of 0.25% and a detection limit of 25.4 mm for water depth, along with an accuracy of 2% for velocity. The device was configured to record water velocity and depth every 30 s. Because the flowmeter could not withstand temperatures below −20°C, it was removed from the site between January 1 and March 31 each year.

Technical issues sometimes made it impossible to communicate with the rain gauge data logger, resulting in the loss of some precipitation data. Similarly, the difficulties related to the flowmeter's accuracy and electrical supply prevented flow rates to be measured at the outlet during certain periods. Despite these difficulties, data were collected for 17 rainfall events (see Table 2). These measurements were used to calculate, for each rainfall event, the proportion of runoff volume leaving the site and the peak flow delay and to build a model describing the hydrology of the site, as described in the following section.

Hydrologic Modeling of the Instrumented Site's Operation

The PCSWMM version 7.0.2340 low-impact development (LID) module (CHI 2018), which is identical to the EPA SWMM5 LID version 5.1.012 module (Rossman and Huber 2016), was used to model the site as a succession of horizontal layers between which water transfers were calculated according to continuity equations specific to each type of stormwater management installation. The permeable pavement sites were represented as four layers, as shown in Fig. 1(b). In the figure, the arrows represent water transfers, which were calculated for every time step according to equations given in Rossman and Huber (2016). Fig. 1 also shows the correspondence between the TB site design and modeling parameters [Fig. 1(a)] and the representation in the LID model in SWMM [Fig. 1(b)].

J. Hydrol. Eng., 2019, 24(8): 05019020

Table 2. Rainfall events and runoff characteristics

Event	Date	Total depth (mm)	Duration (h)	Mean intensity (mm/h)	Maximum 5-min intensity (mm/h)	Runoff/ rain (%)	Peak flow delay (h:min)
#1	2015-10-28	28.0	23.7	1.2	9.6	78	2:45–2:20 (2 peaks)
#2	2015-11-01	8.2	9.7	0.8	26.4	24	0:10
#3	2015-11-06	3.2	1.3	2.5	0.8	4.5	0:04
#4	2015-11-12	20.6	35.0	0.6	12.0	38	0:17
#5	2015-11-27	13.2	13.3	1.0	7.2	26	3:00
#6	2015-12-21	11.8	32.5	0.4	9.6	6	—
#7	2015-12-23	6.8	3.9	1.7	9.6	14	—
#8	2016-07-02	4.6	1.0	4.6	9.6	13	0:13
#9	2016-07-22	5.0	0.5	10.1	19.2	10	0:25
#10	2016-07-23	14.2	3.0	4.8	62.4	68	0:36
#11	2016-07-25	3.0	7.1	0.4	12.0	3	0:21
#12	2016-07-28	1.0	0.1	10.3	9.6	5	0:24
#13	2016-08-16	65.2	12.1	5.4	3.8	108	4:42
#14	2016-08-31	1.4	0.4	3.2	4.8	78	0:27
#15	2016-09-26	4.6	22.5	0.2	0.6	2	0:29
#16	2017-06-12	2.2	0.2	13.2	14.4	4	0:04
#17	2017-08-18	25.8	5.9	4.4	13.0	70	0:51

Table 3. LID parameters for the TB site

Parameter	Type	Value	Limits (for calibration parameters)
Surface layer			
Berm height	Known	150 mm	—
Roughness coefficient (Manning's *n*)	Known	0.013	—
Surface slope	Known	1.14%	—
Pavement layer			
Thickness	Known	100 mm	—
Void ratio	Known	0.4	—
Impervious surface	Known	0.9	—
Permeability	Known	150 mm/h	—
Clogging factor	Negligible	0	—
Soil layer			
Thickness	Known	100 mm	—
Porosity	Known	0.3	—
Field capacity	Calibration	0.110	0.100–0.250
Wilting point	Calibration	0.10	0.01–0.10
Saturated hydraulic conductivity	Calibration	9 mm/h	0–800 mm/h
Conductivity slope	Calibration	19	5–60
Storage layer			
Thickness	Known	508 mm	—
Void ratio	Known	0.4	—
Exfiltration rate	Calibration	0.1 mm/h	0.0–1.3 mm/h
Clogging factor	Negligible	0	—
Underdrain system			
Drain coefficient	Calibration	0.97 mm/h	>0
Drain exponent	Known	0.5	—
Drain offset height	Known	0 mm	—

The LID model parameters for the permeable pavement were divided into three categories: known, negligible, and calibration (see Table 3). The known parameters were those whose values came from site observations, plans, or specifications. The only parameter considered as negligible was the clogging factor (due to the short duration of the simulations). The parameters for model calibration were field capacity, wilting point, saturated hydraulic conductivity, conductivity slope for the soil layer, exfiltration rate, and drain coefficient.

The model was calibrated in three steps: (1) preliminary calibration of the parameters that have an impact on runoff volume; (2) sensitivity analysis; and (3) final calibration. First, values for the exfiltration rate, field capacity, and wilting point parameters were adjusted so as to minimize the square of the relative error between the simulated and observed volume losses (i.e., rainfall volume subtracted from the volume passing through the outlet) for rainfall events 1, 2, 3, 12, and 14 (see Table 2), for which the flowmeter readings were the most reliable.

Second, a sensitivity analysis was conducted using 125 simulations varying the value of each calibration parameter. Parameters were changed one at a time and independently, and their effect on the hydrographs was observed. Last, the value of all calibration parameters was adjusted in order to maximize the Nash-Sutcliffe model efficiency coefficient (Nash and Sutcliffe 1970) between simulated and observed flows and to minimize the relative error between the total simulated and observed volumes at the site's outlet for Events 1 and 13 (see Table 2). These two events were chosen because their duration and total depth were sufficient for presenting a hydrograph curve suitable for calibration purposes, in addition to having different average and maximum rainfall intensities. For this last calibration step, preliminary calibration values were used as starting values for the exfiltration rate, field capacity, and wilting point. Sensitivity analysis results guided the adjustments.

Finally, the calibration results were validated by quantifying the difference between the observed and simulated flows at the site's outfall (Nash-Sutcliffe coefficient and relative error on the total volume) for Event #10, for which the 5-min rainfall intensity was the greatest.

Design Improvement

To improve the hydrologic performance of a PICP site compared with that observed at the TB site, the exfiltration rate, drain offset height, and drain coefficient were modified. The calibration results, along with the results of previous surveys, confirmed that the soil subgrade of the permeable pavement had very low permeability at the TB site; therefore, the site had a low exfiltration rate. In the improved design model, the exfiltration rate was set at 0.12 mm/h, which was still low, even for soils containing clay [for which the exfiltration rate varies from 0.3 to 2.2 mm/h, according to MDDEP and MAMROT (2011)]. At the TB site, the drains were installed directly at the bottom of the structure subbase. Increasing the drain offset height, it was thought, could conceivably result in a longer peak flow delay and possibly increase the amount of water

Fig. 3. Two combined and two separate (industrial) sectors modeled in SWMM.

infiltrating the soil by extending retention (Collins et al. 2008). The drain was, therefore, raised by 50 mm in the improved design. Last, as shown in Fig. 2, drain density in the foundation is very high at the TB site. The drain coefficient is a parameter that combines several drain characteristics and dictates the speed at which the water is evacuated from the permeable pavement's storage layer. In the improved design model, the drain coefficient was reduced by 50% compared with the calibration value, which was equivalent to reducing the drain density by a factor of 2. This modification and raising the drain by 50 mm are both feasible and encouraged by the manufacturer of the pavers, because the TB site has been shown to be overdrained. The only drawback would be a longer emptying time for the storage layer after rain events, but this is usually expected from stormwater source control infrastructure such as PICP sites.

The impact of these three modifications (increase in exfiltration rate, increase in drain offset height, and reduction in drain coefficient) on the total volume and peak flow at the outfall of the TB site, along with the peak flow delay, were evaluated by a SWMM simulation for the calibration and validation rainfalls (Events 1, 10, and 13) (see Table 2).

Modeling of Actual Urban Areas and Impact Assessment

Permeable pavement cells were modeled in four watersheds of a Quebec municipality: two watersheds drained by combined sewer systems and two watersheds drained by separate systems. SWMM simulations were performed for various rainfall scenarios in order to quantify the impact of implementing permeable pavement in an urban area. Fig. 3 shows the locations and SWMM models of the sectors involved. The SWMM models for these sectors had been previously calibrated for the current situation (without PICP) by the city in which the sewer network is located; the city provided the four SWMM models and the rainfall data. In all cases, the permeable pavement was modeled with the LID module using the improved values of the TB site parameters. Table 4 provides a description of the modeled watersheds. For each of the watersheds, SWMM simulations were performed with the following input:

- rainfall series measured at 1-min time steps from May 1 to November 30 for the years 2004–2011 with a rain gauge 5 km from the modeled sectors;
- synthetic rainfalls of the modified Chicago type with a 3-h duration and return periods of 2 and 10 years (used for design purposes in the case study municipality); and
- Events 1, 10, and 13 observed at the TB site (see Table 2).

The following indicators were then calculated:

- for the two watersheds drained by a combined sewer system: reduction in the number, duration, and volume of overflows for scenarios with and without permeable pavement;

Table 4. Description of the four case study urban watersheds

Watershed	Drainage network type	Watershed area (ha)	Permeable pavement area (ha)	Permeable pavement coverage (%)
Industrial 1	Separate	13.7	6.35	46
Industrial 2	Separate	14.4	6.46	45
Combined 1	Combined	5.8	1.52	26
Combined 2	Combined	9.7	1.74	18

- for the two watersheds drained by a separate sewer system: reduction in the peak flows and volumes released at the outfall for scenarios with and without permeable pavement; and
- for the four watersheds: reduction in the duration and frequency of surface flooding for scenarios with and without permeable pavement.

Results and Discussion

Characterization of the Infiltration Capacity of PICP

Infiltration rates were measured at different times during the year, on three occasions for each of the five sites (August 2015; October or November 2015; and May or June 2016), and one additional time at the TB site (February 2016). Test results are presented in Table 1. All results, except one, show an infiltration rate ranging between 698 and 23,121 mm/h (average of 4,044 mm/h; standard deviation of 4,200 mm/h). The only value outside this range (121 mm/h) was a measurement taken at the TB site, very close to a raised border, in an area in which the permeable joints may have become clogged (see the following discussion). However, high-traffic areas showed a high infiltration capacity (e.g., TB2 and TB3, from 1,490 to 3,775 mm/h). It was not possible to correlate the values obtained with the seasons. Infiltration capacities remained very high, even in winter at subzero temperatures (e.g., from −3°C to −5°C in November 2015 and −14°C in February 2016). In addition, due to the similar age of the sites (ranging from 2 to 5 years), it was not possible to study the impact of site age on infiltration capacity or clogging over time.

The infiltration capacities measured were similar to those referred to in previous studies for PICP sites—for example, from 600 to 20,000 mm/h in Bean et al. (2004, 2007); 4,000 mm/h in CIRIA (2007) [cited in Hess and Ibe (2011)]; and more than 1,000 mm/h after 9 years without maintenance in Pratt et al. (1995). In addition, the capacities were all above 250 mm/h (except for the first measurement at TB1), which is the minimum value recommended by the Interlocking Concrete Pavement Institute and the National Concrete Ready Mix Association (Eisenberg et al. 2015). Contrary to what was observed at the five sites in this study, Huang et al. (2016) observed a significant reduction in infiltration capacity in the winter at a PICP site in Calgary (Alberta, Canada). However, that reduction was caused by sand spread on the pavement surface for road maintenance. At the five sites monitored as part of this study, it was observed that spreading sand in winter at the PICP sites would be of little use, because the pavement quickly drains snowmelt; therefore, ice buildup in the winter is very rare.

The low infiltration capacity measured in August 2015 at TB1 (121 mm/h), which borders the PICP site, confirmed the previous results of Braswell et al. (2018), in which it was found that the external contribution in sediments can clog PICP joint. Braswell et al. (2018) evaluated the hydrologic impact of a PICP site installed in series with a biofiltration box (Filterra Bioretention, West Chester, Ohio) in North Carolina for 22 months. Due to the high ratio of impervious area drained to the PICP area (2.6:1), the authors observed significant clogging of the permeable pavement surface in this study. These results show the importance of preventing sediments from outside the PICP site from reaching permeable pavement surfaces. The use of efficient curbs is recommended.

Field Observations and Water Balance at the TB Site

Despite difficulties in measuring flow rates, data was collected for 17 rainfall events. Characteristics of these events are given in Table 2. In the table, runoff/rain corresponds to the runoff volume (integration of the flow measured at the outlet throughout the event) divided by the rainfall volume. Peak flow delay corresponds to the time interval between the occurrence of the maximum rainfall value recorded and the occurrence of the maximum flow rate. For a few of the rainfall events, no peak flow delay was observed because the events were relatively constant.

The results shown in Table 2 reveal that event duration ranged from 0.1 to 35 h, total depth ranged from 1 to 65.2 mm, peak flow delay ranged from 4 min to 4 h 42 min, and percentage of runoff ranged from 2% to 74%. The unrealistic runoff value (108%) for Event #13 can be explained by the fact that flow rate data for this event contained several reading errors that were corrected by replacing missing or atypical values by a linear interpolation between the available values.

The hydrologic monitoring results for the TB site were similar to those of previous studies. Wardynski et al. (2013) measured rainfall for three different PICP cells in the mountains of North Carolina along with the flow rate from these cells over a 7-month period in 2011. Out of the 54 rainfall events with over 2.5 mm of rain recorded during this period, an average runoff reduction of 78%–100% was observed, depending on the cells, with the greatest reduction occurring with cells for which the underdrain was raised in relation to the bottom of the storage layer. Huang et al. (2016) evaluated the storm runoff reduction of three types of permeable pavement, including PICP, in Calgary (Alberta, Canada). Runoff reduction was evaluated during tests in which 4,500 L of water were released from tanks in 20 min onto permeable pavement in order to simulate an 80-mm/h rainfall. The authors observed peak flow reductions ranging from 19% to 64% for PICP and a runoff reduction of 10%–15% for all types of permeable pavements; these low runoff reduction values were most likely related to the very intense simulated rainfall (i.e., the equivalent of 80-mm/h rainfall for 20 min). Winston et al. (2018) monitored rainfall and outlet flow rates over a year and a half at four permeable pavement sites, including three PICP sites, in northern Ohio. The four sites were built on low permeability soils. For the 87 rainfall events recorded during the monitoring period, runoff reduction ranged from 16% to 100% for the PICP sites. No flow rate at the outlets was recorded for 4%–78% of the events, implying a field capacity ranging from 3.0 to 25.2 mm, depending on the site.

Sensitivity Analysis, Calibration, and Validation of the Hydrologic Model for the TB Site

The main observations from the sensitivity analysis conducted with the LID module on the TB site were as follows: (1) when the conductivity slope was low (<18.75, for a 5–60 range), the hydraulic conductivity and the drain coefficient had virtually no effect on outlet flow rates; (2) drain coefficient is the parameter with the greatest impact on the shape of the hydrograph; and (3) several different combinations of values give practically the same hydrograph (equifinality).

The values of parameters estimated during the calibration are given in Table 3. As mentioned previously, the values for the known parameters came from site observations, construction plans, or specifications. The permeability of the pavement layer corresponds to the previously measured infiltration capacity. The observed infiltration capacities at the TB site were all higher than 1,000 mm/h, which means that a rainfall of up to 1,000 mm/h would infiltrate rapidly into the joints without creating any runoff. An arbitrary value of 150 mm/h was entered in the model, because no observed and/or simulated rain events showed a maximal rainfall intensity higher than 150 mm/h. This meant that using a value of

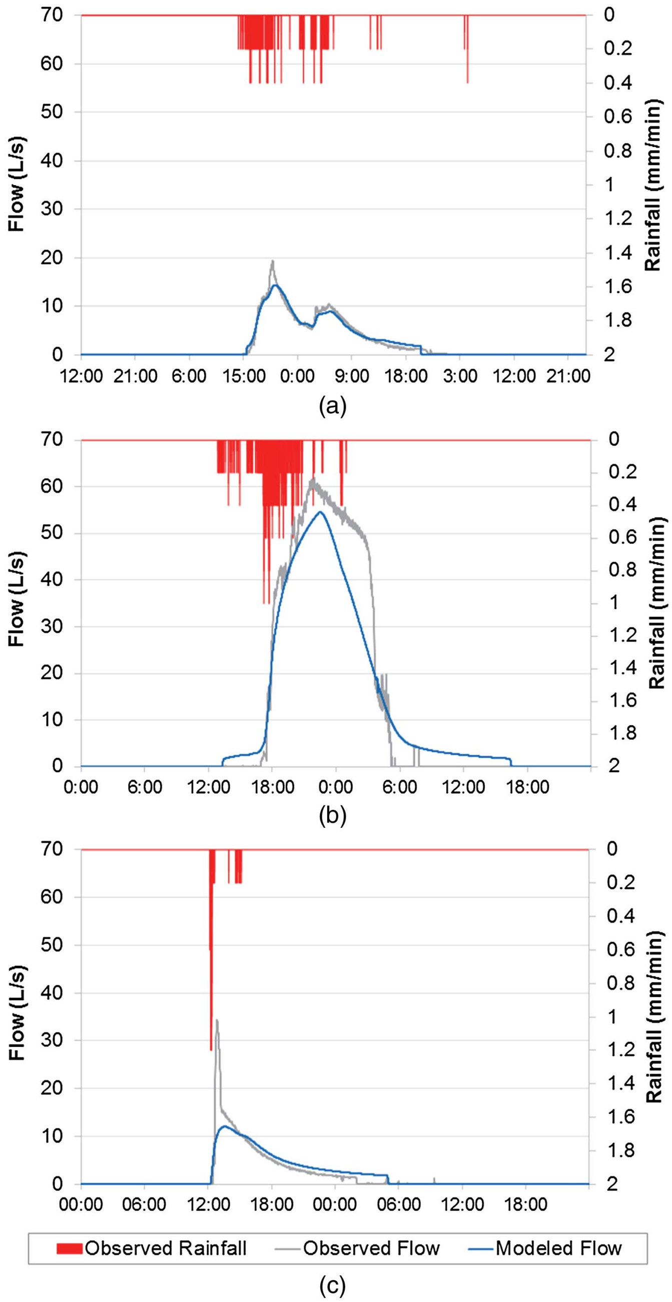

Fig. 4. Flow calibration and validation results: (a) Event #1, October 27–30, 2015 (calibration); (b) Event #13, August 16–17, 2016 (calibration); and (c) Event #10, July 23–24, 2016 (validation).

150 mm/h or higher for the permeability of the pavement layer would result exactly in the same simulated flow at the outlet. The Nash-Sutcliffe coefficients for Event #1 (calibration), Event #13 (calibration) and Event #10 (validation) were 0.97, 0.93, and 0.65, respectively; the squared relative errors for the volumes at the outlet were −2.0%, −8.1%, and 4.7%, respectively, for the same events. Fig. 4 shows the flow rates observed and simulated for Events 1, 10, and 13.

The Nash-Sutcliffe coefficient values were greater than 0.90 for the two calibration events, which shows excellent agreement between the simulated and observed flows rates. The Nash-Sutcliffe coefficient was also very high (0.65) for the validation event, considering that this value was calculated using data observed and simulated at a 1-min time step. The relative error values on the volumes were also low. The simulated flow curves closely followed the rise and fall of the hydrographs observed, except for the peak flow of Event #10, which was underestimated by the model. This discrepancy may have resulted from the very high maximum intensity of rainfall Event #10 (62.4 mm/h over 5 min), which could have caused the flow rate to suddenly rise at the site outlet. The hydrographs in Fig. 4 show that the calibrated model underestimated peak flows. The model should thus be used with caution when estimating the impact of PICP on peak flows and pipe surcharges. However, it is not the main objective of permeable pavement to reduce peak flows significantly, and this underestimation would not have a significant impact on the runoff volume, especially for long rainfall series. Also, it should be recalled that difficulties with the measurements of flows at the outlet of the site were encountered for Event #13. But because, for this event, the main measurement errors occurred during lower flows, the difficulties with the measurements of flows at the outlet of the site should not have an important impact on the calibration results. Finally, because the primary objective of calibrating the LID module at the TB site was to reproduce the average behavior of a permeable pavement unit, the calibration results were deemed appropriate.

Improved Design Model

The hydrologic performance of the improved design model at the TB site, compared with the calibrated model, is shown in Fig. 5. The results identified as "Combination" in this figure are those obtained when the exfiltration rate, the drain offset height, and the drain coefficient were modified simultaneously. Fig. 5 shows that simultaneously modifying these three parameters resulted in a reduction in outfall volume of 27%–100%, depending on the events, a reduction in peak flow of 42%–100%, and a peak flow delay that reached more than 10 h. These improvements were made possible by very conservatively modifying these three parameters—in that increasing drain offset height by 50 mm, reducing the number of drains by half compared with the TB site, and installing the pavement foundation on soil with an infiltration rate of 0.12 mm/h are conditions that can be commonly achieved in practice.

Modeling of Actual Urban Area and Impact Assessment

Fig. 6 summarizes the results regarding (1) reduction in overflows (for combined sewer systems), (2) reduction in flow/volume at the outfall (for separate sewer systems), and (3) reduction in surface flooding duration (for all systems) after adding PICP sites into the four sectors, as modeled by SWMM, for various rainfall scenarios. The reductions identified as "2004–2011" represent the mean reduction for the eight simulated years.

The results in Fig. 6 show a significant reduction in the number, duration, and volume of overflows after adding PICP for the two combined sewer systems and for all modeled rainfall scenarios. Particularly for the 2004–2011 rainfall series, a reduction of 21%–48% in the duration and 26%–65% in the total volume of overflows was noted for each of the combined sewer systems. In the separate sewer systems, the reduction in volume at the outfall for the 2004–2011 series was 30%, and the reduction in peak flow for individual events ranged from 6% to 45%, depending on the sector and the simulated rainfalls. Last, the surface flooding duration for the 2004–2011 series was reduced by 24%–81%, depending on the sector. Despite the two sectors with separate sewer systems having similar overall characteristics (see Table 4), the fact that they have different configurations (see Fig. 3) causes them to have a different hydrologic response.

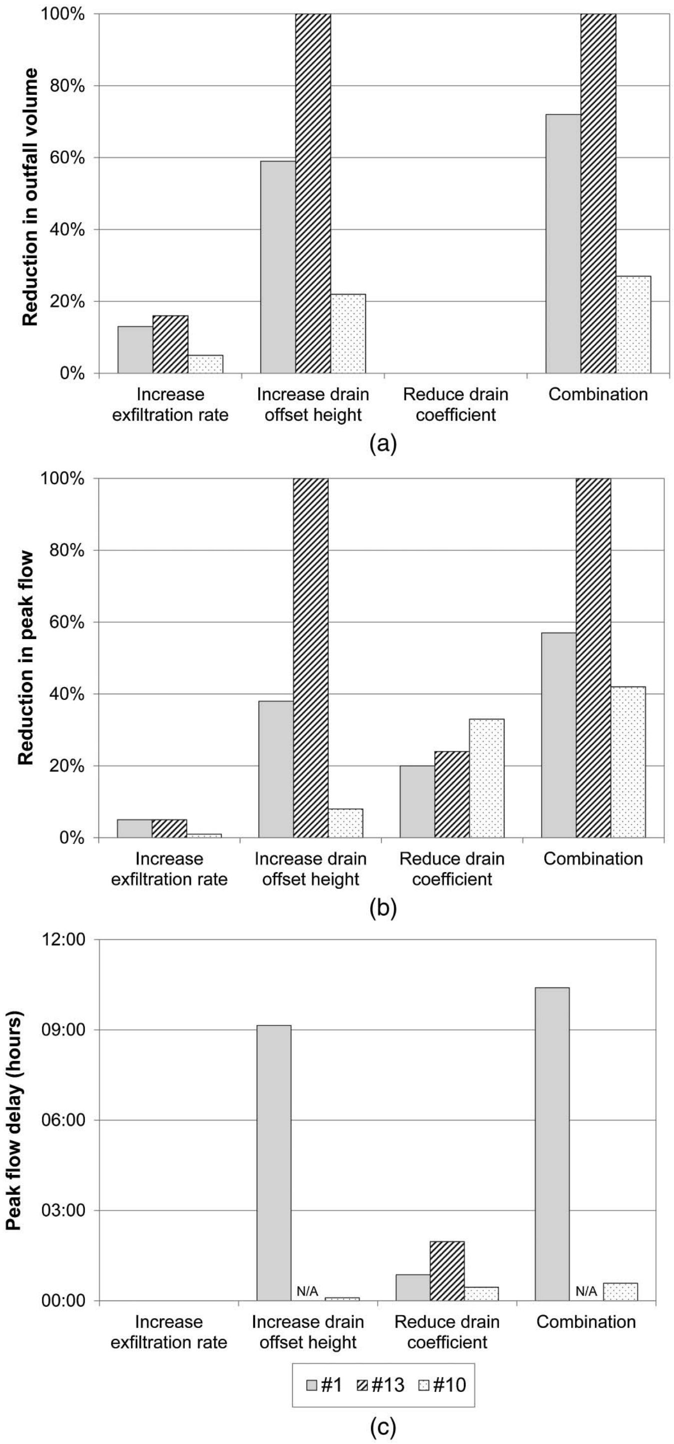

Fig. 5. Results from the improved model at the TB site: (a) reduction in outfall volume; (b) reduction in peak flow; and (c) peak flow delay.

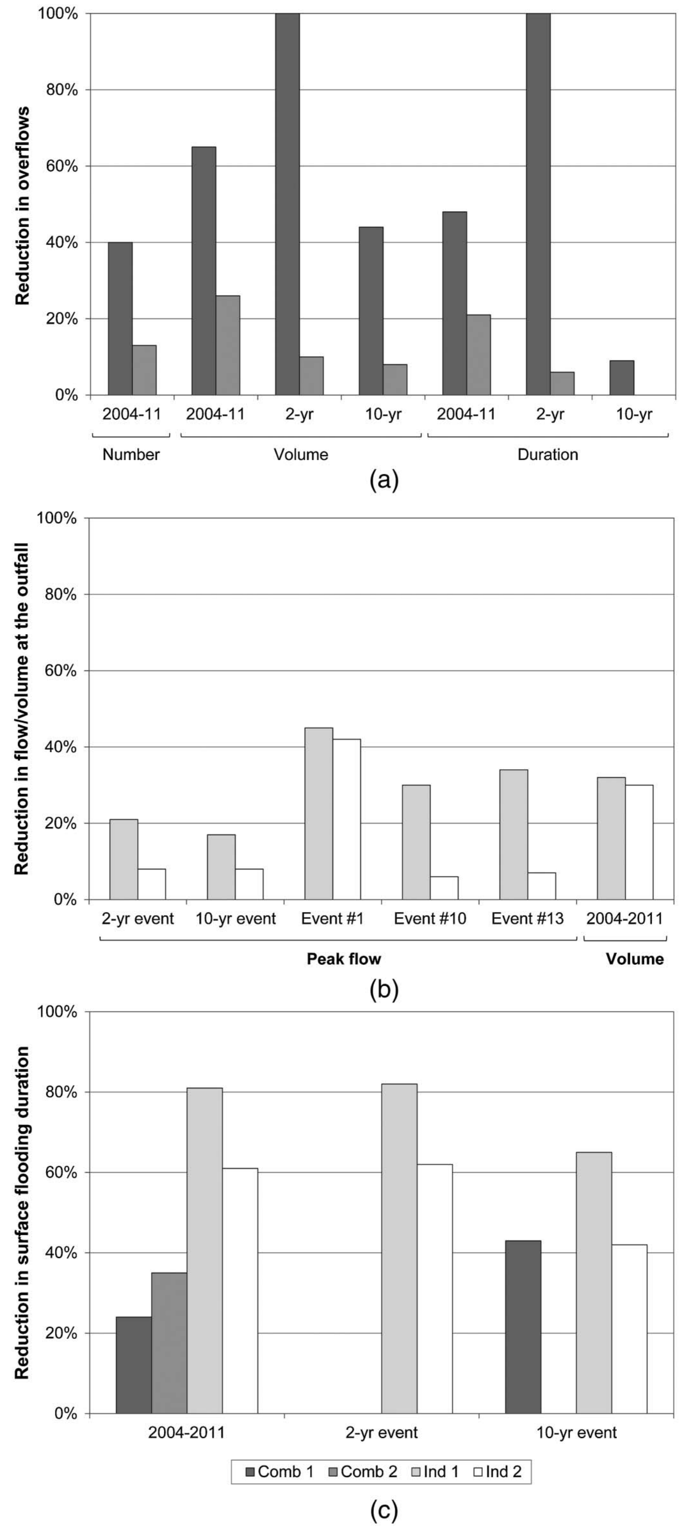

Fig. 6. Results from the improved model: (a) reduction in overflows; (b) reduction in flow/volume at the outfall; and (c) reduction in surface flooding.

These results are similar to those of the only other study to be found on the hydrologic performance of PICP at the subwatershed scale. Hu et al. (2018) evaluated flood risk mitigation by three types of permeable pavement, including PICP, on a 0.58 km^2 and 74% impervious urban watershed. However, in their study, they used a noncalibrated model (default parameters were applied) with only one intense rainfall event (113.8 mm in 12 h, including 83 mm in 2 h). For PICP, they simulated four scenarios (pavement in good or poor condition combined with two storage capacity levels). According to their simulations, these four scenarios led to reductions in peak flow ranging from 12% to 32%.

Conclusion

The main objective of this study was to quantify the impact of implementing PICP in an urban area on the reduction of runoff to watercourses and the reduction of hydraulic malfunctions in storm sewer systems. At the site level, very high surface infiltration rates, up to more than 20,000 mm/h, were observed at five sites in the greater Montreal area (Quebec, Canada), even in winter at subzero temperatures (°C). These infiltration rates were sufficient to avoid surface runoff for the vast majority of rainfall events. Water that seeps through the pavement joints infiltrates a granular material foundation and then leaves the site, either by exfiltration in the soil subgrade or through underdrains to the municipal system. At one of the five monitored sites, the water flow in the drains and the rainfall were monitored for 12 months. This monitoring revealed peak flow delays ranging from 4 min to 4 h 42 min, and a runoff reduction ranging from 26% to 98%, depending on the rainfall event. It should be noted that the instrumented site was implemented on low permeability soil with a densely drained foundation. The site's performance could possibly have been better if it had been on more permeable soil or even if it had the same soil but fewer drains and an increased drain offset height; this was tested through simulations. Rainfall and flow data helped calibrate a PICP hydrologic model, which was used to quantify the impact of implementing PICP in four real urban watersheds.

The simulations showed a reduction in the volume, duration, and number of overflows in the two combined sewer systems, a reduction in peak flows and runoff for the two separate sewer systems, and a reduction in surface flooding duration for all four sectors studied. All results showed the benefits of implementing PICP in urban areas. However, the impact of site age on the infiltration capacity of PICP could not be studied because the tested sites were all about the same age (no more than 5 years). Future work should allow the testing of infiltration rates over several years in order to monitor potential joint clogging and assess how various methods could either prevent clogging or reestablish initial infiltration rates. Technical problems with monitoring equipment also altered the quality of data and the number of rainfall events that could be properly monitored in this study. In the future, monitoring rainfall and flow at various sites would make it possible to assess the impact of different site characteristics (density and position of drains, foundation material, etc.) and therefore guide future designs. More generally, future research should focus on ways to integrate permeable pavement into a global sustainable urban stormwater management strategy that aims to mitigate the impacts of urbanization on receiving bodies of water.

Acknowledgments

The authors gratefully acknowledge the support of Lincoln Paiva from Techo-Bloc and of engineers working for the city that provided the SWMM model and rainfall data that were used for the simulations at the watershed scale. This study was funded by research grants from the Natural Sciences and Engineering Research Council of Canada and from Techo-Bloc. The authors are grateful to Computational Hydraulics Int. for the academic PCSWMM software license.

References

Abbott, C. L., and L. Comino-Mateos. 2003. "In-situ hydraulic performance on a permeable pavement sustainable urban drainage system." *Water Environ. J.* 17 (3): 187–190. https://doi.org/10.1111/j.1747-6593.2003.tb00460.x.

Aryal, S. K., S. Ashbolt, B. S. McIntosh, K. P. Petrone, S. Maheepala, R. K. Chowdhury, T. Gardener, and R. Gardiner. 2016. "Assessing and mitigating the hydrological impacts of urbanisation in semi-urban catchments using the storm water management model." *Water Resour. Manage.* 30 (14): 5437–5454. https://doi.org/10.1007/s11269-016-1499-z.

ASCE. 2018. *Permeable interlocking concrete pavement*. Reston, VA: ASCE.

ASTM. 2015. *Standard test method for surface infiltration rate of permeable unit pavement systems*. ASTM C1781/C1781M-14a. West Conshohocken, PA: ASTM.

Bean, E. Z., W. F. Hunt, and D. A. Bidelspach. 2007. "Field survey of permeable pavement surface infiltration rates." *J. Irrig. Drain. Eng.* 133 (3): 249–255. https://doi.org/10.1061/(ASCE)0733-9437(2007)133:3(249).

Bean, E. Z., W. F. Hunt, D. A. Bidelspach, and R. J. Burak. 2004. "Study on the surface infiltration rate of permeable pavements." In *Proc., 1st Water and Environment Specialty Conf. of the Canadian Society for Civil Engineering*. Montreal: Canadian Society for Civil Engineering.

Beecham, S., D. Pezzaniti, and J. Kandasamy. 2012. "Stormwater treatment using permeable pavements." *Proc. Inst. Civ. Eng. Water Manage.* 165 (3): 161–170.

Braswell, A. S., A. R. Anderson, and W. F. Hunt. 2018. "Hydrologic and water quality evaluation of a permeable pavement and biofiltration device in series." *Water* 10 (1): 33. https://doi.org/10.3390/w10010033.

Brown, R., and M. Borst. 2015. "Nutrient infiltrate concentrations from three permeable pavement types." *J. Environ. Manage.* 164 (1): 74–85. https://doi.org/10.1016/j.jenvman.2015.08.038.

CHI. 2018. "PCSWMM: Advanced modeling software for stormwater, wastewater, watershed and water distribution systems." Accessed September 13, 2018. https://www.pcswmm.com.

CIRIA (Construction Industry Research and Information Association). 2007. *The SUDS manual*, 937. London: CIRIA.

Collins, K., W. Hunt, and J. Hataway. 2008. "Hydrologic comparison of four types of permeable pavement and standard asphalt in Eastern North Carolina." *J. Hydrol. Eng.* 13 (12): 1146–1157. https://doi.org/10.1061/(ASCE)1084-0699(2008)13:12(1146).

Drake, J., A. Bradford, and J. Marsalek. 2013. "Review of environmental performance of permeable pavement systems: State of the knowledge." *Water Qual. Res. J. Can.* 48 (3): 203–222. https://doi.org/10.2166/wqrjc.2013.055.

Drake, J., A. Bradford, and T. Van Seters. 2014a. "Hydrologic performance of three partial-infiltration permeable pavements in a cold climate over low permeability soil." *J. Hydrol. Eng.* 19 (9): 04014016. https://doi.org/10.1061/(ASCE)HE.1943-5584.0000943.

Drake, J., A. Bradford, and T. Van Seters. 2014b. "Stormwater quality of spring-summer-fall effluent from three partial-infiltration permeable pavement systems and conventional asphalt pavement." *J. Environ. Manage.* 139 (Jun): 69–79. https://doi.org/10.1016/j.jenvman.2013.11.056.

Drake, J., A. Bradford, T. Van Seters, and G. MacMillan. 2012. *Evaluation of permeable pavements in cold climates*, 92. Toronto: Toronto and Region Conservation Authority.

Eisenberg, B., K. Collins, and D. Smith. 2015. *Permeable pavements*, 262. Reston, VA: ASCE.

Fassman, E., and S. Blackbourn. 2010. "Urban runoff mitigation by a permeable pavement system over impermeable soils." *J. Hydrol. Eng.* 15 (6): 475–485. https://doi.org/10.1061/(ASCE)HE.1943-5584.0000238.

Fassman, E., and S. Blackbourn. 2011. "Road runoff water-quality mitigation by permeable modular concrete pavers." *J. Irrig. Drain. Eng.* 137 (11): 720–729. https://doi.org/10.1061/(ASCE)IR.1943-4774.0000339.

Fassman, E., and S. Blackbourne. 2007. "Permeable pavement performance for use in active roadways in Auckland, New Zealand." In *Proc., 2nd Low Impact Development Conf.*, 290–306. Reston, VA: ASCE.

Hatt, B. E., T. D. Fletcher, C. J. Walsh, and S. L. Taylor. 2004. "The influence of urban density and drainage infrastructure on the concentrations and loads of pollutants in small streams." *Environ. Manage.* 34 (1): 112–124. https://doi.org/10.1007/s00267-004-0221-8.

Hess, T. M., and C. Ibe. 2011. *Evaluation of the performance of permeable pavement at Lamb Drove: Final*. Cranfield, UK: Dept. of Environmental Science and Technology, Cranfield Univ.

Hu, M., X. Zhang, Y. Siu, Y. Li, K. Tanaka, H. Yang, and Y. Xu. 2018. "Flood mitigation by permeable pavement in Chinese sponge city construction." *Water* 10 (2): 172. https://doi.org/10.3390/w10020172.

Huang, J., C. Valeo, J. He, and A. Chu. 2012. “Winter performance of inter-locking pavers: Stormwater quantity and quality.” *Water* 4 (4): 995–1008. https://doi.org/10.3390/w4040995.

Huang, J., C. Valeo, J. He, and A. Chu. 2016. “Three types of permeable pavements in cold climates: Hydraulic and environmental performance.” *J. Hydrol. Eng.* 142 (6): 04016025. https://doi.org/10.1061/(ASCE)EE.1943-7870.0001085.

Huong, H. T. L., and A. Pathirana. 2013. “Urbanization and climate change impacts on future urban flooding in Can Tho city, Vietnam.” *Hydrol. Earth Syst. Sci.* 17 (1): 379–394. https://doi.org/10.5194/hess-17-379-2013.

ICPI (Interlocking Concrete Pavement Magazine). 2007. “The role of joint filling materials in permeable interlocking concrete pavements.” *Interlocking Concrete Pavement Magazine*, May 16, 2007.

Kim, H., M. Jung, K. J. B. Mallari, G. Pak, S. Kim, S. Kim, L. Kim, and J. Yoon. 2015. “Assessment of porous pavement effectiveness on runoff reduction under climate change scenarios.” *Desalin. Water Treat.* 53 (11): 3142–3147. https://doi.org/10.1080/19443994.2014.922286.

MDDEP and MAMROT (Ministère du Développement durable, de l’Environnement et des Parcs et Ministère des Affaires municipales, des Régions et de l’Occupation du territoire). 2011. *Guide de gestion des eaux pluviales*, 386. [In French.] Québec: MDDEP and MAMROT.

Nash, J. E., and J. V. Sutcliffe. 1970. “River flow forecasting through conceptual models. Part I: A discussion of principles.” *J. Hydrol.* 10 (3): 282–290. https://doi.org/10.1016/0022-1694(70)90255-6.

Neumann, J. E., et al. 2015. “Climate change risks to US infrastructure: Impacts on roads, bridges, coastal development, and urban drainage.” *Clim. Change* 131 (1): 97–109. https://doi.org/10.1007/s10584-013-1037-4.

Pratt, C. J., D. G. Mantle, and P. A. Schofield. 1989. “Urban stormwater reduction and quality improvement through the use of permeable pavements.” *Water Sci. Technol.* 21 (8–9): 769–778. https://doi.org/10.2166/wst.1989.0280.

Pratt, C. J., D. G. Mantle, and P. A. Schofield. 1995. “Research into the performance of permeable pavement, reservoir structures in controlling stormwater discharge quantity and quality.” *Water Sci. Technol.* 32 (1): 63–69. https://doi.org/10.2166/wst.1995.0016.

Rossman, L. A., and W. C. Huber. 2016. *Storm water management model reference manual volume III—Water quality*, 161. Cincinnati: USEPA, Office of Research and Development.

Thelen, E., and L. F. Howe. 1978. *Porous pavement*, 98. Philadelphia: Franklin Institute Press.

TRCA (Toronto and Region Conservation Authority). 2008. *Performance evaluation of permeable pavement and a bioretension swale*, 120. Toronto: TRCA.

Wardynski, B., R. Winston, and W. Hunt. 2013. “Internal water storage enhances exfiltration and thermal load reduction from permeable pavement in the North Carolina Mountains.” *J. Hydrol. Eng.* 139 (2): 187–195. https://doi.org/10.1061/(ASCE)EE.1943-7870.0000626.

Winston, R., J. D. Dorsey, and W. Hunt. 2016. “Quantifying volume reduction and peak flow mitigation for three bioretention cells in clay soils in northeast Ohio.” *Sci. Total Environ.* 553 (May): 83–95. https://doi.org/10.1016/j.scitotenv.2016.02.081.

Winston, R., J. D. Dorsey, A. Smolek, and W. Hunt. 2018. “Hydrologic performance of four permeable pavement systems constructed over low-permeability soils in northeast Ohio.” *J. Hydrol. Eng.* 23 (4): 04018007. https://doi.org/10.1061/(ASCE)HE.1943-5584.0001627.

J. Hydrol. Eng., 2019, 24(8): 05019020